Available online at www.sciencedirect.com

ScienceDirect

MATTER AND RADIATION AT EXTREMES

Matter and Radiation at Extremes 3 (2018) 197–206

www.journals.elsevier.com/matter-and-radiation-at-extremes

Research Article

Development of new diagnostics based on LiF detector for pump-probe experiments

T. Pikuz [a,b,c,*], A. Faenov [b,c], N. Ozaki [a,d], T. Matsuoka [c], B. Albertazzi [a,e], N.J. Hartley [c,f], K. Miyanishi [m], K. Katagiri [a], S. Matsuyama [a], K. Yamauchi [a], H. Habara [a], Y. Inubushi [g], T. Togashi [g], H. Yumoto [g], H. Ohashi [g], Y. Tange [g], T. Yabuuchi [h], M. Yabashi [g,h], A.N. Grum-Grzhimailo [i], A. Casner [j], I. Skobelev [b,k], S. Makarov [b], S. Pikuz [b,k], G. Rigon [e], M. Koenig [a,e], K.A. Tanaka [a,l], T. Ishikawa [g,h], R. Kodama [a,c,d,m]

[a] *Graduate School of Engineering, Osaka University, Suita, Osaka 565-0871, Japan*
[b] *Joint Institute for High Temperatures, Russian Academy of Sciences, Moscow 125412, Russia*
[c] *Open and Transdisciplinary Research Initiatives, Osaka University, Suita, Osaka 565-0871, Japan*
[d] *Photon Pioneers Center, Osaka University, Suita, Osaka 565-0871, Japan*
[e] *LULI – CNRS, École Polytechnique, CEA: Université Paris-Saclay; UPMC Univ Paris 06: Sorbonne Universités - F-91128 Palaiseau cedex, France*
[f] *Helmholtz-Zentrum Dresden-Rossendorf, Dresden 01328, Germany*
[g] *Japan Synchrotron Radiation Research Institute, Sayo-cho, Sayo-gun, Hyogo 679-5198, Japan*
[h] *RIKEN Spring-8 Center, Sayo-cho, Sayo-gun, Hyogo 679-5148, Japan*
[i] *Skobeltsyn Institute of Nuclear Physics, Lomonosov Moscow State University, Moscow 119991, Russia*
[j] *Université de Bordeaux-CNRS-CEA, CELIA (Center Lasers Intenses et Applications), UMR 5107, F-33405 Talence, France*
[k] *National Research Nuclear University MEPhI, Moscow 115409, Russia*
[l] *ELI-NP/IFN-HH, Maqurele-Bucharest 077125 Romania*
[m] *ILE, Osaka University, Suita, Osaka 565-0871, Japan*

Received 20 July 2017; revised 5 January 2018; accepted 8 January 2018
Available online 22 May 2018

Abstract

We present new diagnostics for use in optical laser pump - X-ray Free Electron Laser (XFEL) probe experiments to monitor dimensions, intensity profile and focusability of the XFEL beam and to control initial quality and homogeneity of targets to be driven by optical laser pulse. By developing X-ray imaging, based on the use of an LiF crystal detector, we were able to measure the distribution of energy inside a hard X-ray beam with unprecedented high spatial resolution (~1 μm) and across a field of view larger than some millimetres. This diagnostic can be used *in situ,* provides a very high dynamic range, has an extremely limited cost, and is relatively easy to be implemented in pump-probe experiments. The proposed methods were successfully applied in pump-probe experiments at the SPring-8 Angstrom Compact free electron LAser (SACLA) XFEL facility and its potential was demonstrated for current and future High Energy Density Science experiments.

PACS codes: 41.60.Gr; 61.72Dd; 52.70La; 52.38-r

Keywords: XFEL; Shock waves; Pump-probe experiments; High energy density science; X-ray spectroscopy; X-ray imaging

* Corresponding author. Open and Transdisciplinary Research Initiatives, Osaka University, Suita, Osaka 565-0871, Japan.
E-mail address: pikuz-tatiana@gmail.com (T. Pikuz).
Peer review under responsibility of Science and Technology Information Center, China Academy of Engineering Physics.

https://doi.org/10.1016/j.mre.2018.01.006

1. Introduction

Pump-probe experiment is one of the most informative approaches for receiving unique knowledge about properties of matter under extreme conditions [1−4]. The combination of pulsed power lasers and X-ray Free Electron Laser (XFEL) beams in pump-probe experiments allows insight into the behaviour of solid materials on the timescale of atomic motion, probing ultrafast lattice-level dynamical phenomena and transient states [4−7]. High energy lasers can drive strong shocks by rapidly ablating the surface of a sample, or an ablator layer designed for this purpose. Recently sub-nanosecond or nanosecond laser pulses with intensities 10^{11}−10^{15} W/cm^2 have been used as generators of shock waves, driving pressures from tens of GPa up to multiple TPa. Better understanding of material properties under such conditions is of great interest in different fields including inertial fusion energy research, planetary formation science, and high energy density science. XFELs have allowed *in situ* studies at the lattice-level of matter deformation, melting, and ablation under such extreme pressure for the first time. However, the quality and accuracy of obtained data suffer from a lack of shot-to-shot reproducibility of the experimental data due to the variation in the laser intensity, target quality, and focusing stability. It means that to obtain high quality experimental data in pump-probe experiments, it is necessary to provide monitoring of dimensions, intensity profile and focusability of an XFEL beam used as a probe, as well as quality of targets, driven by optical laser pulses [8]. Presently different methods can be applied for the characterization of XFEL beams. For example, scanning coherent X-ray microscopy or ptychography [9], single-grating interferometry [10], imprinting and ablation method [11], Hartmann method [12] and others are now routinely employed.

In this article, we present new imaging diagnostics based on the use of LiF detectors, which can be easily implemented in experiments to control parameters of XFEL beam and quality of targets with very high spatial resolution within a large field of view.

LiF crystal is a widely used material, in particular as scintillator detector, for different ionizing sources [13]. Recently it is found that LiF is also a very good imaging detector for X-ray radiation [14−21]. Photons with energy greater than 14 eV generate F_2 and F_3^+ type color centers (CCs) in LiF crystals, which are very stable at room temperature. Additionally, these color centers have absorption and emission bands in the visible spectral range, so photoluminescence (PL) of CCs can be observed using conventional fluorescent microscopes. Our investigations have shown that for EUV and soft X-ray radiation the spatial resolution of the PL images can be as low as 700 nm if readout is done using confocal fluorescent microscopes [18] and 75 nm in the case of using scanning near field microscopes [17]. For such radiation, the limit of spatial resolution is mostly defined by the spatial resolution of the microscope system acquiring the readout process. For hard X-ray radiation (spectral range of 5−30 keV), on the other hand, incoming photons generate secondary electrons, causing the creation of color centers inside the crystal throughout the volume of the electron cloud. For example, the size of the electron cloud reaches 1 μm in diameter for 10 keV radiation [21,22] and it becomes even larger for harder photon energies. Consequently, the spatial resolution of LiF detectors at hard X-ray spectral range is defined by the size of the electron cloud. Independent of the spectral range, the LiF detector has a large (at least 10^6) dynamic range. It is not sensitive to visible light and its field of view can be as large as the size of the LiF crystal plate. The unique combination of the properties of the LiF crystal detector allowed significant improvements in capabilities of radiographic technique in X-ray spectral range along with simplification of the experimental setup.

In this article, we discuss the application of LiF detectors for *in situ* single-shot quantitative determination of XFEL beam parameters and describe a novel short-wavelength coherent beam metrology method, based on Fresnel diffraction analysis of high resolution, high dynamic range images (HR-FDA method) [23]. Also we propose the use of an LiF detector to control the quality of targets prior to a pump-probe experiment. In this case, phase contrast and diffraction enhancement in transmission images of thin foils is utilized. At micrometer scale, it allows us to observe structural features of targets in initial condition and changes of target structure under the action of driving optical laser pulse. All the methods mentioned have been successfully applied in pump-probe experiments at the SACLA XFEL facility [21−23].

2. Metrological measurements in pump-probe experiments

As mentioned in Section 1, two types of metrological measurements applied in optical pump-XFEL probe experiments will be discussed below.

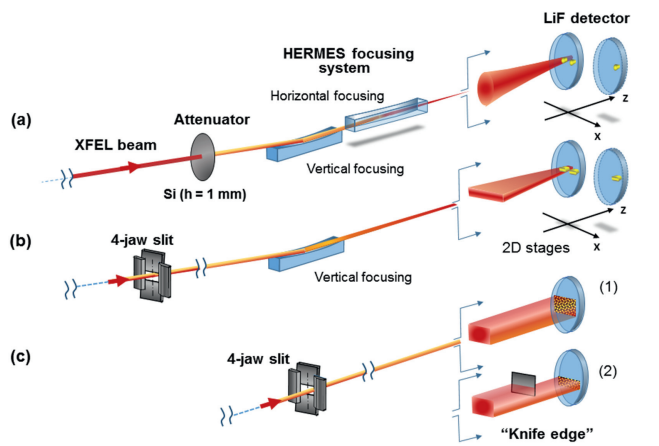

Fig. 1. Schematic views of experiential setup for different type of measurements in experimental hutch EH5 of beam line BL3: (a) 3D visualization of the fully focused XFEL beam; (b) measurement of intensity distribution of the 1D focused XFEL beam along propagation; (c) investigations into the influence of (1) slit dimensions and (2) "knife-edge" on intensity distribution of the direct XFEL beam.

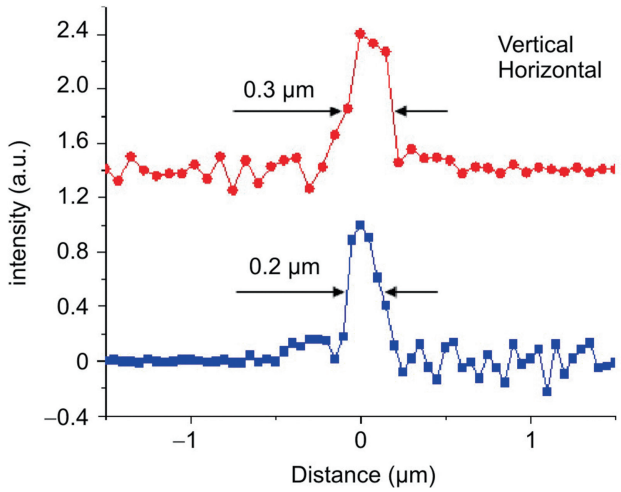

Fig. 2. Intensity profile of XFEL beam focused by HERMES focusing system measured by wire scan method in vertical and horizontal directions (photon energy is 10.1 keV, signal is averaged over 10 shots, energy of beam after attenuation by 1.5 mm Si plate is 0.26 nJ, diameter of gold cross wire is 200 μm).

2.1. In situ, single-shot determination of XFEL beam parameters and focusability

At coherent X-ray radiation facilities, there is an urgent need of simple and efficient methods for *in situ* beamline metrology. Additionally, measurements of energy distribution of XFEL beams within focusing system are very important both for correct evaluation of X-ray fluence in different cross-sections of such beams and for further improving different focusing systems. Here we present X-ray diagnostics based on using LiF X-ray detectors to perform *in situ* measurements on the intensity distribution of X-rays beams with diameters ranging from some microns up to some millimetres with a high spatial resolution (~1 μm). This diagnostic has been applied to characterize the SACLA XFEL beam profile and its focusability.

A sketch of the experimental setup is shown in Fig. 1(a). Experiments have been carried out at the hard X-ray beam line BL3 of the SACLA-SPring-8 facility in experimental hutch EH5 [17]. The XFEL beam was focused to 0.2 μm × 0.3 μm spot by a Kirkpatrick-Baez (KB) type HERMES focusing system onto the surface of the LiF crystal detector. Fig. 2 presents the intensity profiles of the focus spot measured by a wire-scan method in vertical and horizontal directions.

The operating principle of an LiF crystal detector is as follows: the crystal is exposed to the X-ray radiation, which generates CCs. Particular CCs have an absorption band from 440 to 480 nm and a photo-emission band (photo-luminescence) in the visible spectral range, which allows the readout of the images using commercial microscopes such as confocal fluorescence microscopes. The high sensitivity and large dynamic range of the LiF crystal detector allows intensity distributions at distances far from the best focus as well as near the best focus to be measured (See Fig. 3(a) and (b)). We would like to underline that the dynamic range of the LiF detector was enough to observe not only the XFEL beam itself but also the projection of the focusing system aperture. PL images in Fig. 3(a) show the presence of small shift of XFEL beam from the center of the aperture which takes place in this particular experiment. Thus alignment of XFEL axis on the mirrors of the focusing system can also be controlled.

Intensity distribution in cross sections of XFEL beam was measured at relatively long distance of 17.5 mm around the focus. This sequence of PL images was used to reconstruct the caustic of the focused beam and to provide evaluation of the XFEL source size and beam propagation factor M^2. It was also found that the actual position of the focus was 5 mm away

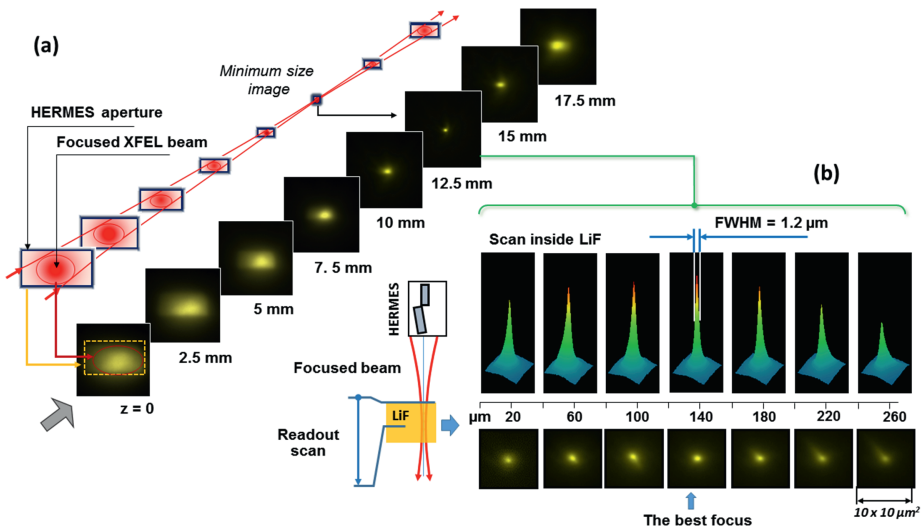

Fig. 3. Intensity distribution of focused XFEL beam near the focal position [21]: (a) sequence of PL image of XFEL beam, obtained on the LiF detector surface by scanning along the propagation direction with step of 2.5 mm, and schematic interpretation of images (above); (b) observation of PL caused by XFEL beam in the volume of LiF at the position of minimum image size ($Z = 12.5$ mm). The coordinate of Z is defined in Fig. 1(a and b). Sketch on the left hand side shows the range of measurements inside the crystal; below there are PL images, measured at different distances from the surface of the LiF crystal. The spatial distribution of the PL intensity for each image is shown above. The best focus is indicated by a blue arrow.

from the predicted location. At the same time, the smallest measured size of the focal spot was of order ~1.0 μm, which is larger than the one mentioned above. Analysis of this result allowes to conclude that our measurements well support the theoretical prediction that for photons with energies of ~10 keV, the diameter of the generated photoelectron cloud in LiF reaches ~1000 nm before thermalization [21,22].

In many pump-probe experiments, the size of the X-ray probe beam should be comparable to the size of the optical laser focal spot, i.e. of the order of a few hundreds of microns. In such cases, to have high probe beam intensity on the target, the XFEL beam is focused in one direction while in the second direction, the size of beam is set by selecting the 4-jaw slit equal to the size of the pumping optical laser beam focal spot (See Fig. 1(b)).

The LiF crystal detector was used in such pump-probe experiments at SACLA XFEL facility to determine the position along the beam axis with optimal sizes and to control the quality of the focused beam. It was found that at the beginning of the experiment, a local damage on Kirkpatrick mirror distorted the focused beam (See Fig. 4). After the damaged part of the mirror was moved out of the beam, the probe beam profile was improved containing a diffraction pattern only (See the inset in Fig. 4). The obtained quality of the XFEL beam allowed us to successfully provide pump-probe experiments [4,7]. We would like to stress that distortions and diffraction patterns in the XFEL beam were clearly resolved in the single-shot XFEL transmission images.

2.2. A novel short-wavelength coherent beam metrology method for single-shot quantitative determination of XFEL beam parameters

Diffraction of X-ray laser beams is widely used for a variety of different measurements. At the same time, the potential of diffraction methods for beamline metrology has not been yet fully exploited because the diffraction fringes are very often separated by only a few microns or even less, and their intensity drops dramatically with increasing fringe number. This means that usually they could not be resolved with ordinary pixel- and luminosity-limited detectors. A two dimensional (2D) procedure based on high-resolution Fresnel diffraction analysis is discussed and applied in Ref. [23], which allowed an efficient and detailed beamline characterization at the SACLA XFEL facility.

Fig. 1(c) shows a conceptual sketch of the experimental set-up, while Fig. 5 demonstrates the images obtained in the case of using various rectangular field masks. Self-amplified spontaneous emission (SASE) occurs about the virtual source position of XFEL beam, which then propagates until

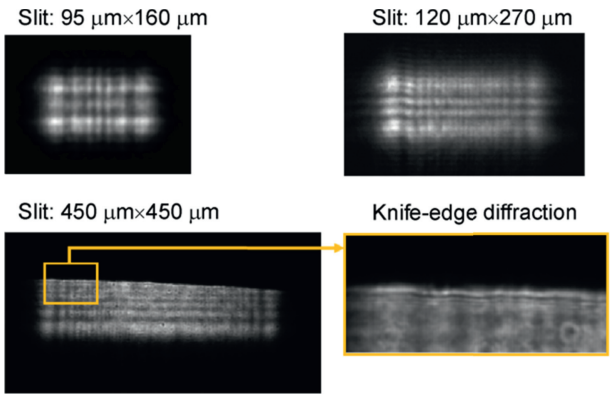

Fig. 5. *In situ* registration of intensity distribution of the XFEL probe beam, limited by a rectangular aperture. Diffraction patterns in the position of the target for different sizes of 4-jaw slit are shown. In the inset, the diffraction fringes formed by the knife-edge obstacle, which is placed closer to the LiF detector than the slit are clearly resolved. The distance from 4-jaw slit to the detector is 8.3 m; the distance from knife-edge to the detector is 150 mm.

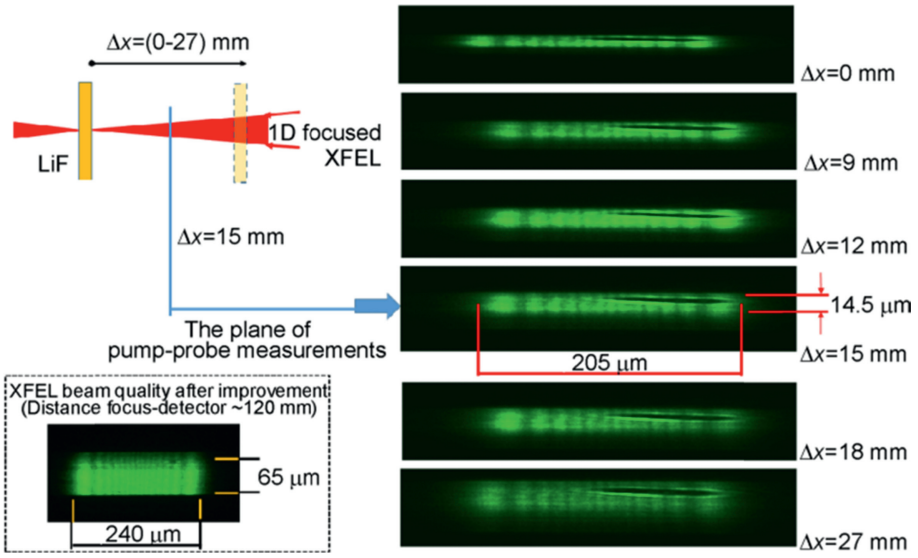

Fig. 4. Intensity distribution of XFEL beam, vertically focused and dimensionally limited by the horizontal slit of 200 μm. Selected images were obtained on the LiF detector at different cross sections of the beam near the focal plane (see scheme in the upper left). The plane with beam dimensions required for target probe ($\Delta x = 15$ mm) was determined with high accuracy. Diffraction pattern and local destruction of beam quality by tiny obstacle located on the focusing mirror is clearly seen. The inset shows the high quality of the XFEL beam after improvement of mirror quality.

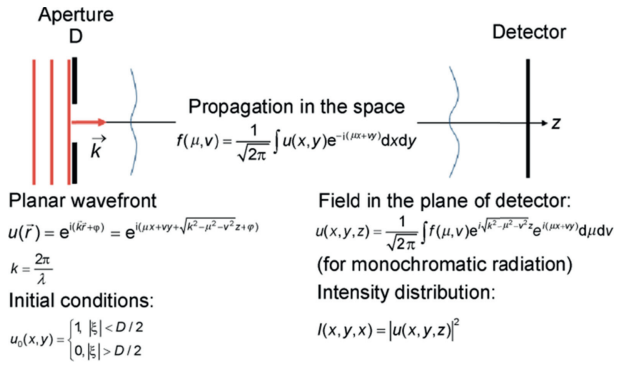

Fig. 6. Schematic presentation of algorithm, used for modelling XFEL beam intensity distribution in the plane of detector for experimental scheme (3) (see Fig. 1 (c)).

meets the probe-mask and is diffracted by it. The diffraction from the probe-mask was monitored at distance $L_d = 8.3$ m from the aperture of the mask, which was close enough to the detector to produce a Fresnel diffraction pattern (see Fig. 5). The intensity patterns were obtained *in situ* from a single-shot and acquired with an LiF crystal imaging detector, that is LiF plate with diameter of 20 mm and thickness of 2 mm. A photon energy $E_{ph} = 10.1$ keV was used, which is well above the LiF cutoff sensitivity of 14 eV. The pulse energy of the XFEL beam at the exit of the undulator was E ~400 μJ (2.5×10^{11} photons). In Fig. 5 the high-spatial frequency imaging capability of an irradiated LiF crystal detector is clearly seen. Very tiny details of diffraction patterns are obviously resolved, which allow 2D information of the coherence degree, beam divergence, beam quality factor M^2, pointing stability of the beam in vertical and horizontal directions and the size of virtual source to be retrieved.

The experimental patterns were analysed with a computational method which reproduced their shape for a given set of initial beamline parameters. The analysis was based on calculating the wave equation using the Fourier transform algorithm. The basic idea of algorithm is schematically presented in Fig. 6. A self-written iterative code was applied to convolute the theoretical patterns and different Gaussian illumination functions, to find the least residuals to the experimental results (see Fig. 6). A very good overlap of experimental and modelled results was obtained and it is clearly seen for both horizontal and vertical directions of the rectangular slit (see Fig. 7).

We would like to stress that the discussed method can be accurately realized in a single-shot measurements due to high dynamic range of LiF detector. Ordinary and compact equipment is required. Thus it can be easily implemented for characterization and optimization of probe beam. As was mentioned above, in the context of High Energy Density (HED) research, an XFEL beam can be used as a probe to obtain information on material properties and/or on atomic scale processes with an unprecedented time resolution. In most of these experiments [1–4], a slit was located in the path of the XFEL beam at various distances from the zone of pump-probe investigations to control the size of the beam from tens to hundreds of microns. It means that due to a very high degree of XFEL beam coherence, the initial distribution of beam intensity passing through the optical channel will be

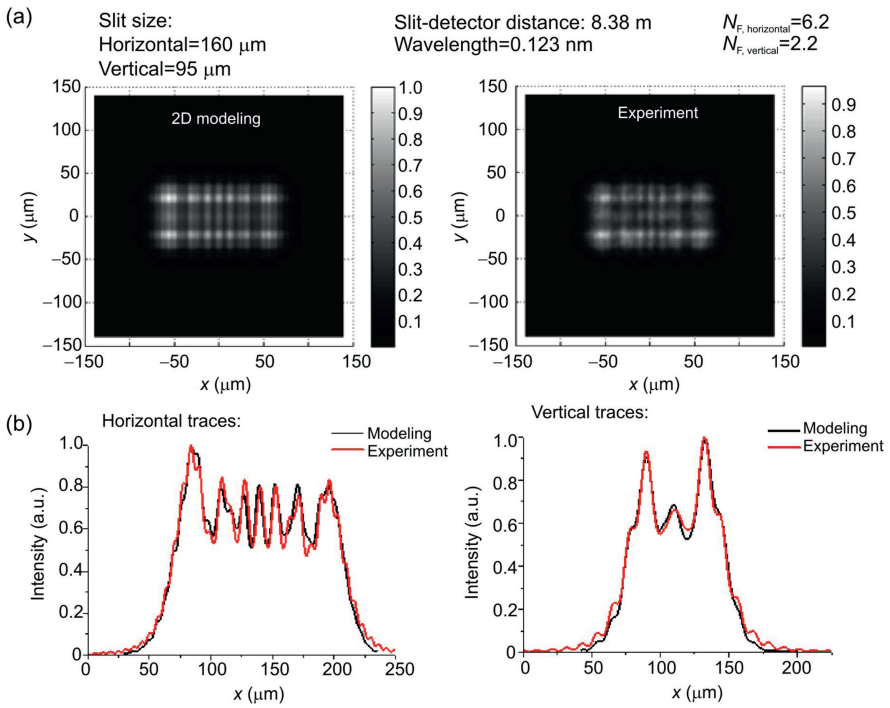

Fig. 7. (a) Result of 2D modelling and experimental diffraction patterns at the position of the target for the XFEL beam limited by a slit with a size of 160 μm (horizontal) × 95 μm (vertical); (b) comparison of theoretical and the experimental intensity distributions in horizontal and vertical directions. Almost perfect agreement of traces confirms a high degree of beam coherence.

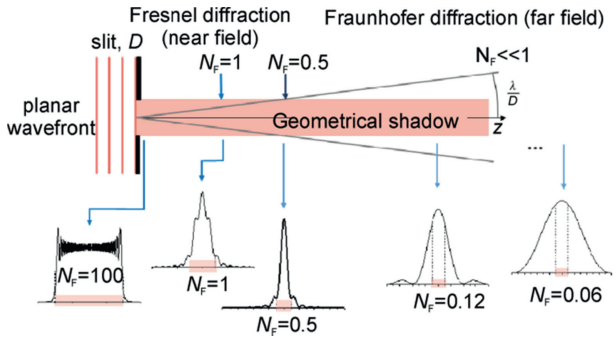

Fig. 8. Evolution of the diffraction patterns for the monochromatic planar wave propagated through the slit with increasing the distance between the 4-jaw slit and the detector, which caused transformation from Fresnel diffraction ($N_F > 1$) to Fraunhofer diffraction ($N_F << 1$). The dimension of slit shadow is shown in pink.

disturbed by any aperture, the 4-jaw slit, obstacle or micro-defects on the surface of optical components and, in particular, on the surface of the focusing system. When coherent wavefronts are incident on the aperture, the intensity distribution (diffraction patterns structures) in the propagated beam strongly depends on the distance from the aperture to the plane of the detector (See Fig. 8). The shape of the intensity distribution on the detector will be similar to the aperture shape only at a distance of a few wavelengths from the aperture. With the increase of the distance from the aperture to the detector, the intensity distribution in the beam will transfer to Fresnel diffraction pattern. With further increase of the distance to the detector, a Fraunhofer diffraction pattern occurs. The general criterion for describing a particular diffraction regime is the Fresnel number $N_F = a^2/(Z\,\lambda)$, where a is the aperture radius, Z is the aperture-detector distance and λ is the XFEL wavelength. The diffraction patterns for monochromatic planar wave propagated through the 4-jaw slit evolve with the increase of the distance to the slit from Fresnel diffraction ($N_F > 1$) to Fraunhofer diffraction ($N_F << 1$) as shown in Fig. 8. Fresnel diffraction is characterized by the appearance of large numbers of diffraction fringes near the edges of the slit image and the size of image is close to the size of the slit width. In the Fraunhofer regime, the size of the beam is different to the shape of the slit. The intensity distribution in the pattern becomes pure diffraction with size much greater than the slit size. In Fig. 8, the size of the slit aperture relative to the diffraction pattern is shown by the pink rectangular areas. Usually experimental conditions require to use XFEL beam with specific dimensions in one or both (horizontal and/or vertical) directions, which causes different inhomogeneities in the beam aperture.

Characterizing the level of such inhomogeneous energy distribution inside the X-ray beam with high spatial resolution (less than 1 μm) is challenging but necessary. Indeed, several studies already show that this characterization has a key role in the success of XFEL experiments. For example, knowledge of the homogeneity of the X-ray beam is essential to undertaking useful comparison between molecular dynamics (MD) simulations and experimental results while avoiding large error bars on experimental data. On the other hand, studies of ultrafast elastic–plastic transition [1] need a spatially uniform probe to avoid strong inhomogeneities in the Debye–Scherrer cone, as the detector generally only observes part of the ring, while still being able to compare the experimental results to simulations.

As mentioned above, the LiF crystal X-ray detector could be effectively used for the characterization of XFEL beam quality (See Figs. 3–5), but experimental measurements are

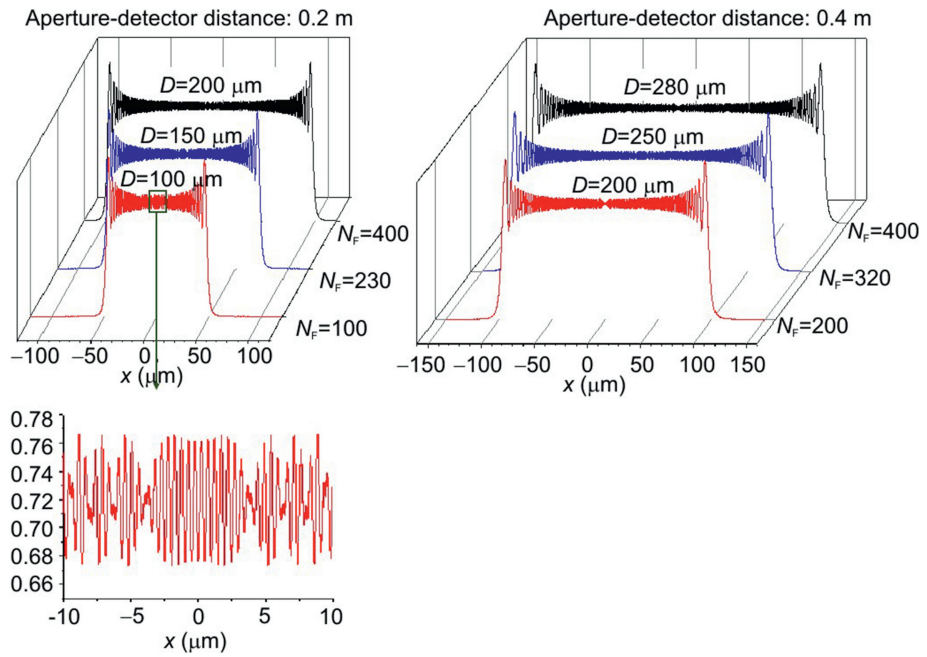

Fig. 9. Near field (Fresnel diffraction) XFEL beam intensity distribution *vs* Fresnel number at distances from the slit, modelled for monochromatic radiation (10.1 keV).

time consuming. It is very useful to know in advance the influence of beam diffraction on the beam homogeneity for different sizes of stop aperture and distances from the object. In Figs. 9–11, the results of the beam propagation modelling for different distances between the aperture and the detector and for different sizes of the aperture are presented in the Fresnel diffraction case. In this regime ($N_F >> 1$), the intensity distribution of the monochromatic beam is highly modulated (clearly seen in the enlarged part of the red traces in Figs. 9 and 10). Increasing the Fresnel number leads to a quasi-homogeneous intensity distribution (particularly in the central part of the beam) with high frequency oscillations, which are not so strongly affect the experimental conditions in most cases. We also could see that the size of the beam is similar to the size of the aperture despite the effect of diffraction.

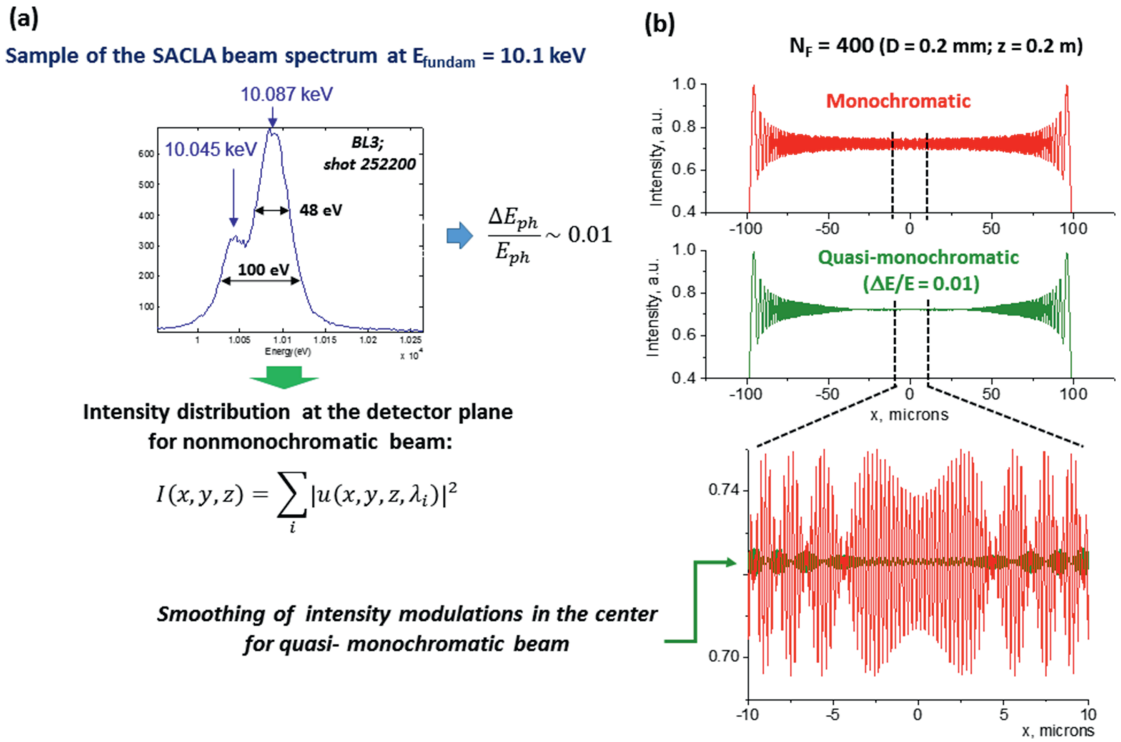

Fig. 10. Modelling of near field (Fresnel diffraction) XFEL beam intensity distribution by taking into account real spectral bandwidth of XFEL pulse: (a) a sample SACLA XFEL spectrum with a fundamental photon energy of 10.1 keV; (b) comparison of calculated intensity distributions for monochromatic and quasi-monochromatic radiation with $N_F = 400$.

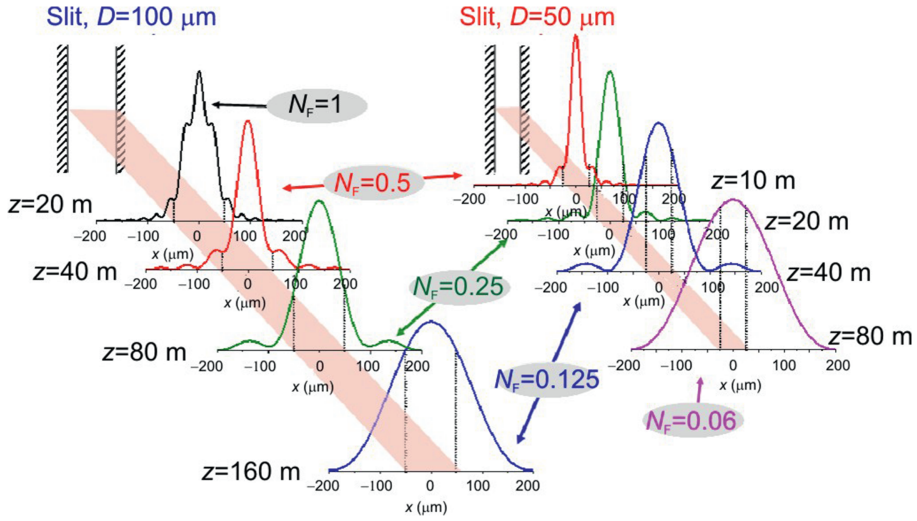

Fig. 11. Far field (Fraunhofer diffraction) XFEL beam intensity distribution vs Fresnel number at two sizes of slit; modelling for monochromatic radiation (10.1 keV).

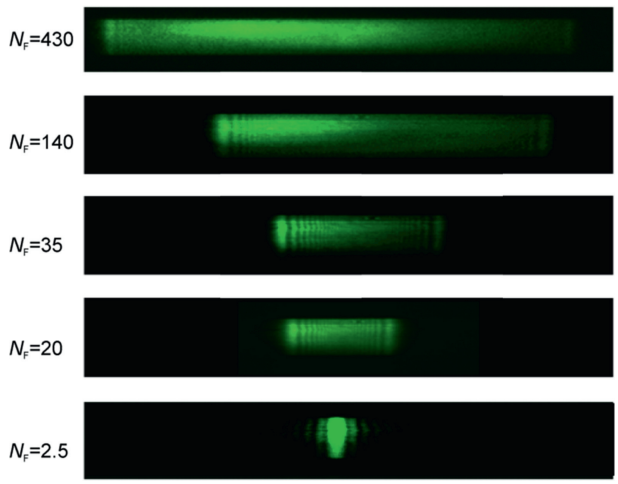

Fig. 12. XFEL beam intensity distribution on dependence of Fresnel number (slit-detector distance is 8.3 m).

In the case of Fraunhofer diffraction (large distances between the aperture and detector), as could be seen from Fig. 11, the diffracted beam is generally more smooth. This effect is more pronounced in the central zone of the propagated beam. Unfortunately the major drawback of using Fraunhofer diffraction in pump-probe experiments is the need to place the aperture very far (usually at >10 m) from the detector, then the consequent increase in the beam size will lead to a decrease in intensity.

The experimental dependence of intensity distribution of the SACLA XFEL beam on the size of the slit is presented in Fig. 12. The photon energy is 10.1 keV and the slit is located at 8.3 m from the center of the pump-probe experimental chamber. On the left side of each image, a corresponding Fresnel number is shown.

3. Proof of principle of target quality control in optical laser pump-XFEL probe HEDS experiments by high spatial resolution X-ray imaging

For high precision pump-probe measurements, it is necessary to control not only the homogeneity of the pump and probe beams, but also the homogeneity and quality of the targets. To reach this goal, it is very important to measure the target quality directly before the pump-probe experiment. Our experiments at the SACLA XFEL facility demonstrated that such single shot *in situ* control is possible using LiF crystal detectors (See Fig. 13). Indeed, differences between targets are clearly resolved in single-shot XFEL transmission images. These inhomogeneities could be observed for targets with a wide range of X-ray transmissivities: 50 μm CH + 10 μm Al (80% transmission at 10.1 keV), 5 μm (Si + Cu) (5% transmission), 10 μm Fe (2% transmission) and even 5 μm Ta (0.3% transmission). Significant differences in structure for targets made from the same material (marked in Fig. 13 as (a)–(b) or (a)–(c)) were also found. Such a large dynamic range is unique for detectors used in the hard X-ray energy range. We applied the proposed technique in pump-probe experiment to observe structural transformation of targets driven by the pump laser pulse (Fig. 14). The experiment was carried out as follows. The LiF crystal was placed ~120 mm behind the target. Thin target foil consisted of 30 μm layer of polypropylene and 40 μm of Ge. Subsequently ten XFEL probe pulses with an energy of 400 μJ (photon energy of 10.1 keV, repetition rate of 1 Hz, attenuated much below the ablation threshold of the target) were sent to the target. The inclination of the target to the axis of the XFEL beam was 24°. Each of the ten transmission images of the target was measured by the LiF crystal. Randomly, one of the XFEL pulses (No.07 in the experiment) was synchronized with the pump laser pulse. Obtained images clearly show the scenario

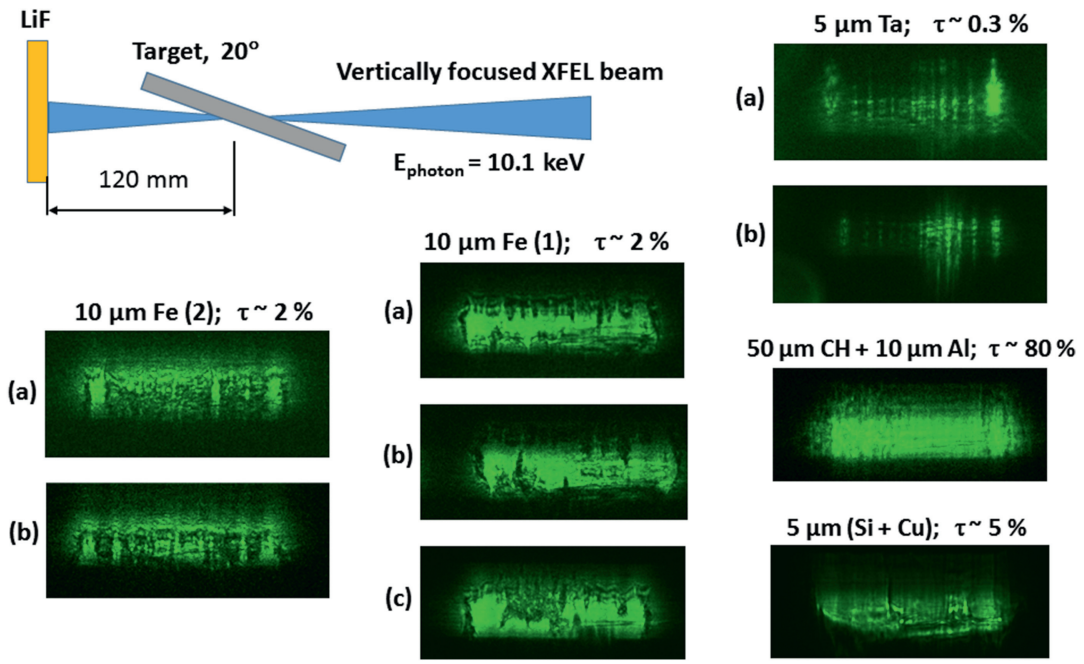

Fig. 13. Control of pump-probe targets homogeneity: experimental setup and single-shot transmission images of targets made from different materials.

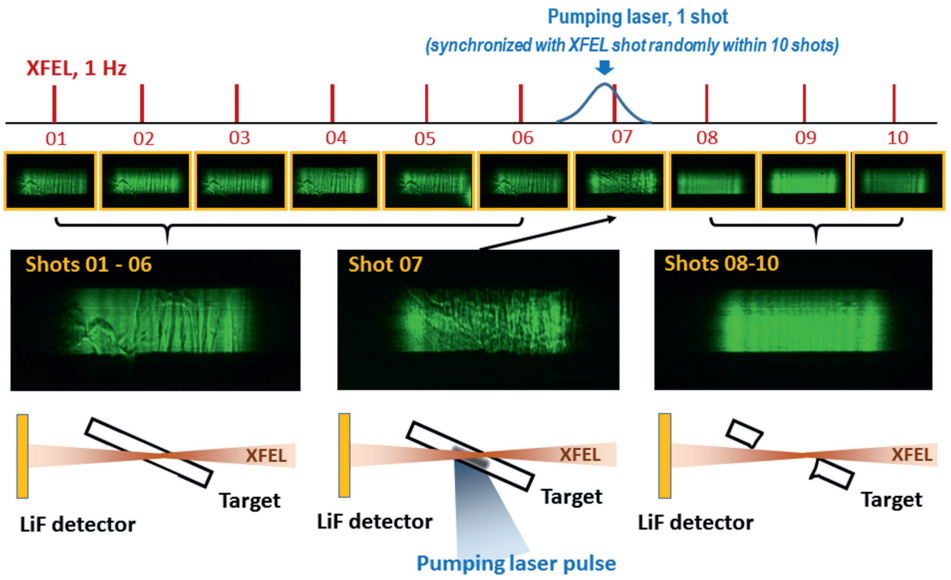

Fig. 14. High resolution transmission imaging for observation of a volume structure transformation of a thin target driven by a single pump laser pulse.

of measurements. During the first six shots, XFEL pulses illuminated the target, which kept the initial condition, therefore images 01–06 were similar and initial structural inhomogeneities of the target were well resolved. During XFEL shot No.07, the coming pump laser pulse completely changed the internal structure of the target. As the optical pump laser finally destroyed the target, three more XFEL pulses freely propagated through the target hole. Images obtained during XFEL shots 08–10 show only the structure of the XFEL beam itself.

4. Conclusion

We have developed a package of diagnostics to be used for metrological control of different parameters in optical laser pump-XFEL beam probe experiments. They provide single shot *in situ* metrology of the hard XFEL probe beam characteristics and XFEL beam focusability, allowing single-shot transmission imaging for controlling the quality of targets in such experiments to be performed. All of these methods have been successfully applied in pump-probe experiments at the SACLA XFEL facility. We would like to stress that the X-ray diagnostics presented here, all based on the use of an LiF crystal X-ray detector, are able to measure the distribution of energy inside an X-ray beam *in situ*, with high spatial resolution (~1 μm) for a beam diameter larger than a few millimetres. The diagnostics have an extremely limited cost, which are relatively easy to set up and can be used to provide information on the uniformity of the X-rays beam on a shot-to-shot basis. A first observation using this diagnostic at EH5 in SACLA shows that the presence of an upstream slit leads to a highly structured XFEL beam due to the generated diffraction pattern.

Conflict of interest

The authors declare no competing financial or non-financial interests.

Acknowledgements

The XFEL experiments were performed at the BL3 of SACLA with the approval of the Japan Synchrotron Radiation Research Institute (JASRI) (Proposals Nos. 2014A8045, and 2014B8068). This research was partially supported by grants from Grants-in-Aid for Scientific Research (Kakenhi Grant Nos. 15H02153 and 17K05729) and the Core-to-Core Program on International Alliance for Material Science in Extreme States with High Power Laser of the Japan Society for the Promotion of Science (JSPS), from the X-ray Free Electron Laser Priority Strategy Program of the MEXT, contract 12005014, and within the state assignment of FASO of Russia (theme № 01201357846). The part of work was supported by the Agence Nationale de la Recherche in the frame of the ANR project TurboHEDP (ANR-15-CE30-0011).

References

[1] D. Milathianaki, S. Boutet, G.J. Williams, A. Higginbotham, D. Ratner, et al., Femtosecond visualization of lattice dynamics in shock-compressed matter, Science 342 (2013) 220–223.
[2] J. Gaudin, C. Fourment, B.I. Cho, K. Engelhorn, E. Galtier, et al., Towards simultaneous measurements of electronic and structural properties in ultra-fast X-ray free electron laser absorption spectroscopy experiments, Sci. Rep. 4 (2014) 4724.
[3] C.R.D. Brown, D.O. Gericke, M. Cammarata, B.I. Cho, T. Döppner, et al., Evidence for a glassy state in strongly driven carbon, Sci. Rep. 4 (2014) 5214.
[4] B. Albertazzi, N. Ozaki, V. Zhakhovsky, A. Faenov, H. Habara, et al., Dynamic fracture of tantalum under extreme tensile stress, Science Advances 3 (2017), e1602705.
[5] B.K. McFarland, N. Berrah, C. Bostedt, J. Bozek, P.H. Bucksbaum, et al., Experimental strategies for optical pump-soft X-ray probe experiments at the LCLS, J. Phys. Conf. 488 (2014) 012015.
[6] S. de Jong, R. Kukreja, C. Trabant, N. Pontius, C.F. Chang, et al., Speed limit of the insulator–metal transition in magnetite, Nat. Mater. 12 (2013) 882–886.

[7] N.J. Hartley, N. Ozaki, T. Matsuoka, B. Albertazzi, A. Faenov, et al., Ultrafast observation of lattice dynamics in laser-irradiated gold foils, Appl. Phys. Lett. 110 (2017) 071905.
[8] M. Yabashi, H. Tanaka, T. Ishikawa, Overview of the SACLA facility, J. Synchrotron Radiat. 22 (2015) 477−484.
[9] A. Schropp, R. Hoppe, V. Meier, J. Patommel, F. Seiboth, et al., Full spatial characterization of a nanofocused X-ray free-electron laser beam by ptychographic imaging, Sci. Rep. 3 (2013) 1633. www.nature.comientificreport.
[10] S. Matsuyama, H. Yokoyama, R. Fukui, Y. Kohmura, K. Tamasaku, et al., Wavefront measurement for a hard-X-ray nanobeam using single-grating interferometry, Optic Express 20 (2012) 24977−24986.
[11] J. Chalupský, P. Boháček, T. Burian, V. Hájková, S.P. Hau-Riege, et al., Imprinting a focused X-ray laser beam to measure its full spatial characteristics, Phys. Rev. Applied 4 (2015) 014004.
[12] B. Floter, P. Juranic, P. Großmann, S. Kapitzki, B. Keitel, et al., Beam parameters of FLASH beamline BL1 from Hartmann wavefront measurements, NIMA 635 (2011) S108−S112.
[13] J.H. Schulman, W.D. Compton, Color Centers in Solids, Oxford, Pergamon, 1962.
[14] G. Baldacchini, F. Bongfigli, F. Flora, R.M. Montereali, D. Murra, et al., High-contrast photoluminiscent patterns in lithium fluoride crystals produced by soft X-rays from a laser-plasma source, Appl. Phys. Lett. 80 (2002) 4810−4812.
[15] G. Baldacchini, F. Bongfigli, A. Faenov, F. Flora, R.M. Montereali, et al., Lithium fluoride as a novel X-ray image detector for biological μ-world capture, J. Nanosci. Nanotechnol. 3 (2003) 483−486.
[16] G. Baldacchini, S. Bollanti, F. Bonfigli, F. Flora, P. Di Lazzaro, et al., Soft X-ray submicron imaging detectors based on point defects in LiF, Rev. Sci. Instrum. 76 (2005) 113104.
[17] A. Ustione, A. Cricenti, F. Bonfigli, F. Flora, A. Lai, et al., Scanning near-field optical microscopy images of microradiographs stored in lithium fluoride films with an optical resolution of $\lambda/12$, Appl. Phys. Lett. 88 (2006) 141107.
[18] A. Ya. Faenov, Y. Kato, M. Tanaka, T.A. Pikuz, M. Kishimoto, et al., Submicrometer-resolution *in situ* imaging of the focus pattern of a soft X-ray laser by color center formation in LiF crystal, Optic Lett. 34 (2009) 941−943.
[19] T. Pikuz, A. Faenov, Y. Fukuda, M. Kando, P. Bolton, et al., Optical features of a LiF crystal soft X-ray imaging detector irradiated by free electron laser pulses, Optic Express 20 (4) (2012) 3424−3433.
[20] T.A. Pikuz, A. Ya. Faenov, Y. Fukuda, M. Kando, P. Bolton, et al., Soft X-ray Free-Electron Laser imaging by LiF crystal and film detectors over a wide range of fluences, Appl. Optic. 52 (2013) 509−515.
[21] T. Pikuz, A. Faenov, T. Matsuoka, S. Matsuyama, K. Yamauchi, et al., 3D visualization of XFEL beam focusing properties using LiF crystal X-ray detector, Sci. Rep. 5 (2015) 17713.
[22] A.N. Grum-Grzhimailo, T. Pikuz, A. Faenov, T. Matsuoka, N. Ozaki, et al., On the size of the secondary electron cloud in crystals irradiated by hard X-ray photons, Eur. Phys. J. D 71 (2017) 69.
[23] M. Ruiz-Lopez, A. Faenov, T. Pikuz, N. Ozaki, A. Mitrofanov, et al., Coherent X-ray beam metrology using 2D high-resolution Fresnel-diffraction analysis, J. Synchrotron Radiat. 24 (2017) 196−204.